

## Structural, Thermal, and Optical Properties of GeO<sub>2</sub>-La<sub>2</sub>O<sub>3</sub>-TiO<sub>2</sub> Glasses

WAN Jiabao<sup>1</sup>, ZHANG Minghui<sup>2</sup>, SU Huaiyu<sup>2</sup>, CAO Zhijun<sup>2</sup>, LIU Xuechao<sup>2</sup>,  
XIE Jiansheng<sup>2</sup>, WANG Xiangyuan<sup>2</sup>, SHI Yinghui<sup>2</sup>, WANG Liang<sup>2</sup>, LEI Shuijin<sup>1</sup>

(1. School of Physics and Materials Science, Nanchang University, Nanchang 330031, China; 2. Shanghai Institute of Ceramics, Chinese Academy of Sciences, Shanghai 200050, China)

**Abstract:** La<sub>2</sub>O<sub>3</sub>-TiO<sub>2</sub> glasses show promising application prospect in fields of lenses, optical windows, and optical communication, owing to their high refractive index and excellent performance. However, this glass cannot be prepared into large size because of its weak glass forming ability, which seriously limits its application. In this study, introducing the network former GeO<sub>2</sub> can effectively improve the glass forming ability, so that large-sized GeO<sub>2</sub>-La<sub>2</sub>O<sub>3</sub>-TiO<sub>2</sub> (GLT) glass can be prepared using conventional methods. Differential thermal analysis shows that GLT glasses have high glass transition temperature ( $T_g$ ) and strong resistance to precipitation, with  $T_g$  and  $\Delta T$  ( $T_{c-onset}-T_g$ ) greater than 833 and 209 °C, respectively. The refractive index is up to 2.06. The transmittance can reach 78% in the visible and near-infrared wavelength bands. The glass forming ability and thermal stability can be weakened by increasing the content of TiO<sub>2</sub>. The molar volume and oxygen electron polarizability exhibit the same variation trends as the refractive index of the samples. This result is important for developing new devices with high performance, light weight, and small size.

**Key words:** high refractive index; thermal stability; large size glass; high transmittance

Owing to the miniaturization and lightweight of optical devices, the requirement of optical glasses with high refractive index has increased gradually. New heavy-metal oxide glass materials exhibit high thermal stability and high refractive index, which have been widely studied and applied in lenses and optical windows<sup>[1]</sup>. Glasses with high refractive index can effectively reduce the volume of optical components and increase the viewing angle<sup>[2]</sup>. In optical design, optical glasses with refractive index between 1.9 and 2.2 are of great significance for simplifying optical systems, improving imaging quality, and miniaturizing devices. In addition, high refractive index glasses can be used in short-wave infrared detection equipment<sup>[3]</sup>, semiconductor integrated circuit chip short-wave lithography<sup>[4]</sup>, camera lenses, tank fire control system driver perimeter mirrors<sup>[5]</sup>, etc. Therefore, new heavy-metal oxide glasses with high refractive index and large size are paid more and more attention.

La<sub>2</sub>O<sub>3</sub>-TiO<sub>2</sub> glasses fabricated by aerodynamic levitation are widely studied for high refractive index. TiO<sub>2</sub> shows high refractive index and plays an important role in the field of high refractive-index glasses. The advantages of lanthanum-containing glasses are the unique combination of high refractive index, low dispersion, and high transparency over a wide range of wavelengths<sup>[6]</sup>. In 2008, Arai, *et al.*<sup>[6]</sup> fabricated La<sub>4</sub>Ti<sub>9</sub>O<sub>24</sub> glass spheres with refractive index of 2.37 at 587 nm. It is proved that high refractive index of La<sub>4</sub>Ti<sub>9</sub>O<sub>24</sub> is due to high concentration of titanate and high volume ratio of TiO<sub>5</sub> clusters. In the La<sub>4</sub>Ti<sub>9</sub>O<sub>24</sub> glass structure, 65% of the TiO<sub>5</sub> polyhedra and 35% of the TiO<sub>6</sub> polyhedra coexist. Compared with the TiO<sub>6</sub> polyhedra, the TiO<sub>5</sub> polyhedra in the glasses greatly improves the polarizability, which endows the La<sub>4</sub>Ti<sub>9</sub>O<sub>24</sub> glass with high refractive index properties<sup>[7]</sup>. Titanium dioxide exists in complex forms in glasses, with the forms of 4, 5, and 6 coordination in the glass network structure<sup>[8]</sup>. In

**Received date:** 2023-02-10; **Revised date:** 2023-02-24; **Published online:** 2023-03-23

**Foundation item:** National Natural Science Foundation of China (21961019, 22265018); Chinese Academy of Sciences (2020256); Science and Technology Committee of Shanghai (20QA1410300, 22511100300, 20511107400); Space Utilization System of China Manned Space Engineering (KJZ-YY-NCL07); National Key Research and Development Program of China (2021YFA0716304)

**Biography:** WAN Jiabao (1998–), male, Master candidate. E-mail: jbwana\_siccas@126.com  
万家宝(1998–), 男, 硕士研究生. E-mail: jbwana\_siccas@126.com

**Corresponding author:** LEI Shuijin, professor. E-mail: shjlei@ncu.edu.cn; ZHANG Minghui, associate professor. E-mail: zhangminghui@mail.sic.ac.cn  
雷水金, 教授. E-mail: shjlei@ncu.edu.cn; 张明辉, 副研究员. E-mail: zhangminghui@mail.sic.ac.cn

addition, Farges, *et al.*<sup>[9]</sup> revealed the existence of oxygen quadruple, quintuple, and hexaplet clusters in titanium silicate compositions. Adding titanium dioxide to glasses can improve optical property, even obtain ultra-high refractive index<sup>[10-11]</sup>. Titanium dioxide may play a leading role in the optical properties and structure of titanate-based glass.

La<sub>2</sub>O<sub>3</sub>-TiO<sub>2</sub> glasses with refractive index more than 2.0 are mostly prepared by containerless processing methods<sup>[12-13]</sup>. However, the glasses prepared by such methods are too small to be applied. Generally, the diameter of glass spheres prepared by containerless methods does not exceed 10 mm<sup>[14]</sup>, which limits the applications in large-size optical lenses, tank perimetry, infrared windows, *etc.* By hot-pressed sintering, large-size lanthanum titanium glass can be prepared. However, because the glass prepared by this method is too colored and has a maximum transmittance of 54% in the visible light region<sup>[14]</sup>, it cannot be used as a material for the preparation of optical lenses and windows. Therefore, in order to obtain large-size high-refractive index lanthanum titanium optical glass, it is meaningful to find a suitable network former and locate a balance point between size and high refractive index, and prepare large-size high-refractive index lanthanum titanium optical glass by high-temperature melting method. To date, large-size La<sub>2</sub>O<sub>3</sub>-TiO<sub>2</sub> based glasses with high refractive index by high temperature melt quenching method has not been reported<sup>[15]</sup>. Based on the containerless lanthanum-titanium binary glass system, the glass forming ability can be improved by introducing GeO<sub>2</sub>. Germanate glasses can dissolve a large number of rare earth ions<sup>[16]</sup>. Moreover, GeO<sub>2</sub> exhibits a high refractive index<sup>[17]</sup>. Therefore, GeO<sub>2</sub>-La<sub>2</sub>O<sub>3</sub>-TiO<sub>2</sub> glasses with large size and high refractive index can be prepared by high temperature melt quenching method. Structural, optical and thermal property of the new glasses would be studied.

## 1 Experimental

The compositions of new glasses are determined to be (0.74-*x*)GeO<sub>2</sub>-0.26La<sub>2</sub>O<sub>3</sub>-*x*TiO<sub>2</sub> (*x*=0.45, 0.47, 0.49, 0.51, 0.53), labeled as GLT-(1-5). High purity GeO<sub>2</sub> (99.99%, in mass), La<sub>2</sub>O<sub>3</sub> (99.99%, in mass), and TiO<sub>2</sub> (99.99%, in mass) powders were weighted, and fully mixed according to stoichiometric composition. 10% (in mol) H<sub>3</sub>BO<sub>3</sub> (99.99%, in mass) was added into the mixture, as a melting aid. EDS results show that the boric acid can volatilize completely at this melting temperature and holding time. For each sample, a 20 g batch of raw

materials was thoroughly mixed and then melted in muffle furnace (VSF1700) at 1300 °C for 5 h in platinum crucible. Then, the melt was cast into a copper mold at high temperature to obtain bulk glasses. The glass samples were then placed in a muffle furnace pre-heated to about 50 °C below the glass transition temperature  $T_g$  (about 790 °C) for 5 h to eliminate the internal residual stress and oxygen vacancy. Glass samples with diameter of larger than 20 mm and thickness greater than 5 mm were successfully prepared. The glasses were then reduced to a thickness of 1.5 mm by double-sided polishing for follow-up tests.

The glass transition and initial crystallization temperatures were measured by a thermal analysis mass spectrometer STA449C (DTA, STA449C, FEI, USA) at a heating rate of 10 °C/min. Raman spectra were obtained by a laser Micro-Raman spectrometer (Thermo Scientific DXR) excited by a 633 nm incident laser. X-ray Diffraction (XRD) was performed using an X-ray diffractometer (Brooke D8ADVANCE, Germany). The density was measured in a gas pycnometer (Micromeritics AccupycII1340, Atlanta, Georgia). Optical transmittance spectra were measured using an ultraviolet spectrophotometer (Cary 5000) in the wavelength range from 250 to 2000 nm. Transmittance spectra in the range of 2000-10000 nm were detected by a Fourier-transform infrared spectrometer (EQUINOX55). Refractive index curves were measured and fitted by ellipsometry (J.A. Woollam M2000) in the range of 210-1600 nm.

## 2 Results and discussion

### 2.1 Thermal property

The thermal stability can be indicated by the temperature difference  $\Delta T = T_x - T_g$ , where  $T_x$  is the crystallization onset temperature and  $T_g$  is the glass transition temperature<sup>[18]</sup>.  $\Delta T$  reflects the resistance of the glass phase to crystallization during the heat-treatment<sup>[19]</sup>. The DTA curves of GLT-(1-5) glasses are shown in Fig. 1(a). Owing to the existence of a large exothermic peak, the glass transition temperature  $T_g$  and crystallization peak  $T_p$  can be easily obtained from the results. Fig. 1(b) depicts an enlarged view of the  $T_g$  areas of the GLT glasses.  $T_g$ ,  $T_x$ , and  $\Delta T$  are evaluated from DTA curves. The curves are plotted with the content of TiO<sub>2</sub> as variable in Fig. 1(c). As shown in Fig. 1(c),  $T_g$  grows gradually as TiO<sub>2</sub> is added. The maximum  $\Delta T$  is about 236.1 °C at 45% (in mol) TiO<sub>2</sub>, as shown in the inset of Fig. 1(c).

The results show that the glass forming ability and

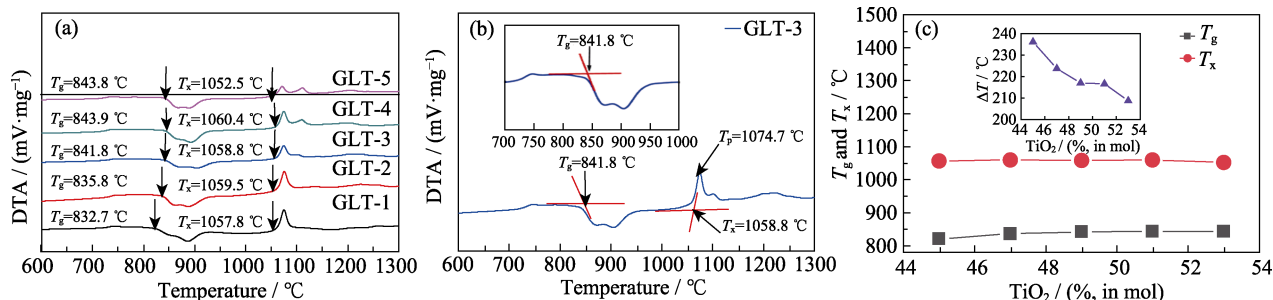


Fig. 1 DTA curves of GLT(1-5) glasses

(a) DTA curves of the GLT(1-5) glasses; (b) DTA curve of the GLT-3 glass with inset showing an enlarged view of the glass transition; (c) Glass transition temperature  $T_g$  and crystallization onset temperature  $T_x$  varied with the change of the glasses composition with inset showing the difference of  $\Delta T$  ( $\Delta T = T_x - T_g$ )

thermal stability can be weakened by increasing the content of  $\text{TiO}_2$ . As  $\text{TiO}_2$  content is more than 54% (in mol), or less than 45% (in mol), GLT glasses cannot be prepared. Therefore, 49% (in mol)  $\text{TiO}_2$  is the optimal addition for the glass stability.

## 2.2 Glass structure

A series of GLT glasses with different titanium contents were prepared by high temperature melting. The XRD patterns of the glass samples obtained by traditional melting method are presented in Fig. 2, indicating that the glasses are colorless and transparent. The absence of characteristic peaks in the XRD patterns indicates amorphous structure. In high temperature environment at 1300 °C, a redox equilibrium reaction of titanium ions occurs in glasses, which is  $\text{TiO}_2 \rightarrow \text{TiO}_{2-x} + x/2\text{O}_2 + \text{XO}^{2-}$ . This coloration-induced equilibrium is influenced by the acidity and alkalinity of the glass, melting atmosphere, and melting temperature. The presence of  $\text{Ti}^{4+}$  in the sample causes  $\text{Ti}^{4+}$  ion to strongly absorb ultraviolet light and to absorb the purple-blue part of the band in the visible region, which can make the glass yellowish coloration<sup>[20]</sup>.

The network structure is studied by Raman spectra. Fig. 3 shows the Raman spectra of the GLT(1-5) glasses. The peak characteristics of different chemical bonds are

marked in the spectra, near 120, 300 and 760  $\text{cm}^{-1}$ . As the content of  $\text{TiO}_2$  increasing, the peak around 300  $\text{cm}^{-1}$  shifts from 294 to 315  $\text{cm}^{-1}$ , and then moves back to 298  $\text{cm}^{-1}$ . The peak intensity decreases after GLT-4 reaches maximum. The laws of the peaks near 120 and 760  $\text{cm}^{-1}$  are similar.

The peaks at 120  $\text{cm}^{-1}$  may correspond to the boson peak, which is a universal feature of disordered materials<sup>[21-22]</sup>. In addition, the wide peak at 300  $\text{cm}^{-1}$  corresponds to the vibration mode of the interconnected  $\text{GeO}_6$  polyhedra<sup>[23]</sup>. The hump at 760  $\text{cm}^{-1}$  is caused by two non-bridging oxygen atoms (Ge-O-NBO) of the  $\text{GeO}_4$  tetrahedron<sup>[24]</sup> and  $\text{TiO}_n$  including titanium oxide quadruple, quintuple, and hexaplet clusters<sup>[8]</sup>. The lower peak of the binding energy is NBO, and the higher binding energy is bridging oxygen (Bridging Oxygens, BOs). The lower the amount of non-bridging oxygen, the higher the stability of the glass network structure and the tighter the connectivity of the structural units are. In general, three valence states of Ti are present in  $\text{TiO}_n$  clusters simultaneously. Because the proportion of the  $\text{TiO}_4$  polyhedra is much lower than those of  $\text{TiO}_5$  and  $\text{TiO}_6$ , it contributes little to the overall structural change. In addition, the proportion of  $\text{TiO}_6$  decreases with an

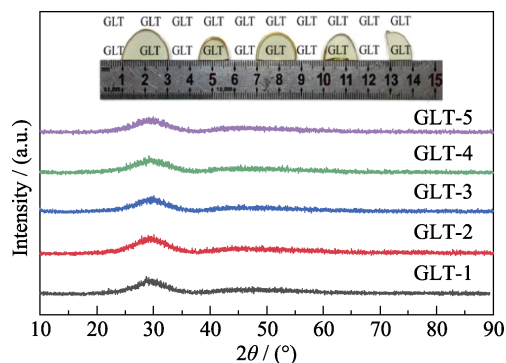


Fig. 2 XRD patterns of GLT(1-5) glasses

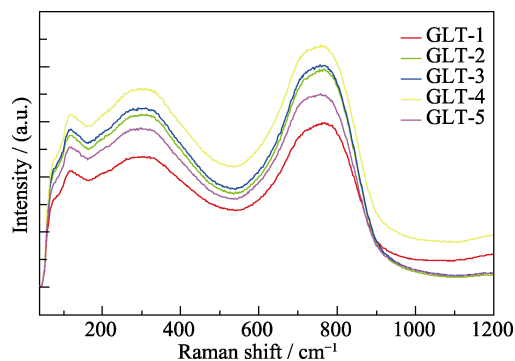


Fig. 3 Raman scattering spectra of GLT(1-5) glasses at room temperature

Colorful figure is available on website

increase in the Ti content, and a portion of TiO<sub>6</sub> is transformed into the TiO<sub>5</sub> structure. By increasing the length of the Ti–O bond and the proportion of TiO<sub>5</sub>, the TiO<sub>*n*</sub> polyhedral structure becomes denser<sup>[18]</sup>.

### 2.3 Optical properties

Fig. 4 shows the optical transmittance spectra of GLT-(1–5) glass in the visible to mid-infrared range. The glasses show almost no absorption in the visible region, and the maximum transmittance of each sample is greater than 72%. The highest transmittance reaches 78% in GLT-1 glasses. The theoretical transmittance can be calculated by the formula  $T=(1-R)^2$  and  $R=(n-1)^2/(n+1)^2$ , where  $R$  is the reflection coefficient and  $n$  is the refractive index. The actual test value of 78.01% is completely consistent with the theoretical transmittance of 78.36% calculated by the above formula. The maximum transmittance of glasses decreases slightly with the increase of TiO<sub>2</sub> content, which is due to the difference in the reflection coefficient caused by different refractive indices. With refractive index increasing, the corresponding transmittance decreases. Fig. 4(b) shows the infrared transmission spectra of GLT glasses. The cutoff wavelengths determined at 5% transmission of GLT-(1–5) glasses are 3.733.77 μm.

The main absorption band near 2.9 μm may be caused by the existence of free hydroxyl (OH) groups<sup>[25]</sup>. The calculation formula of hydroxyl absorption coefficient is  $\alpha_{OH}=\ln(T_0/T)/L$ , where  $L$  is the thickness of the glass sample,  $T$  is the transmittance of the absorption band at 3000 nm, and  $T_0$  is the maximum infrared transmittance of the glass sample.

The calculated absorption coefficients of the GLT-(1–5) glasses are 3.36, 3.22, 3.20, 3.32, and 3.33 cm<sup>-1</sup>. The uncertainty for absorption coefficient is affected by the test accuracy of transmittance and sample thickness. The uncertainty is ±0.01.

The cutoff wavelength at 5% transmittance in the IR region was slightly changed from 3.75 μm for GLT-1 glass to 3.73 μm for GLT-5 glass. Compared with silicate and borate glasses, the cutoff wavelength of GLT glasses are shorter. These changes can be attributed to the vibrational energy of phonons. The maximum phonon energy of the sample is 765 cm<sup>-1</sup>, so that the infrared absorption edge of the samples are shorter than that of other oxide glasses such as the silicate and borate glasses<sup>[26-27]</sup>.

The refractive index increases gradually to the maximum value of 2.06 and then tends to stabilize. When

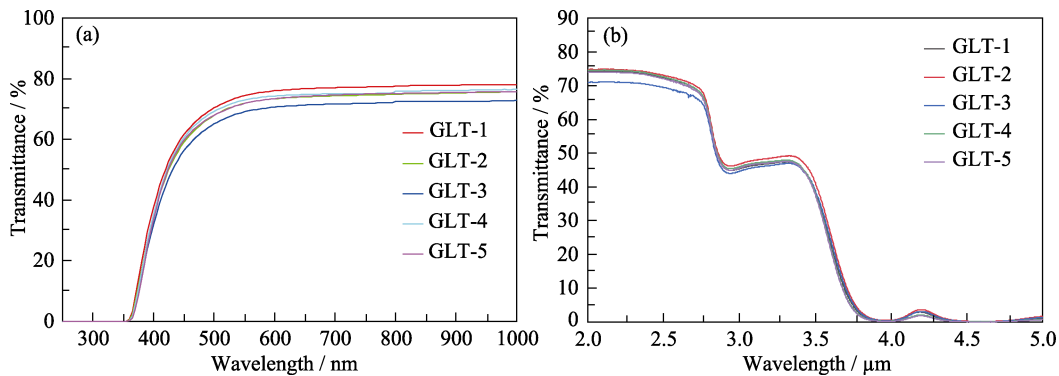


Fig. 4 Optical transmittance spectra of GLT-(1–5) glasses

(a) UV-Vis; (b) MIR region

Colorful figures are available on website

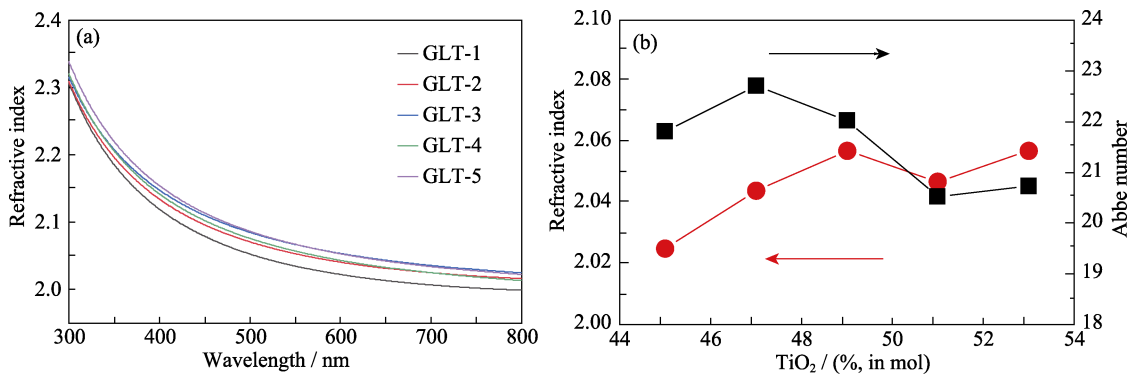


Fig. 5 Refractive index curves (a) of GLT-(1–5) glasses at 300–800 nm wavelength, the dependence

(b) of refractive index  $n_d$  and Abbe number on the TiO<sub>2</sub> content

Colorful figures are available on website

TiO<sub>2</sub> replaces GeO<sub>2</sub>, the refractive index increases because TiO<sub>2</sub> with refractive index of 2.55 is higher than GeO<sub>2</sub>. The refractive index of GeO<sub>2</sub> is only 1.99<sup>[28]</sup>. Since the high refractive index of titanium dioxide has a great influence on the performance, the refractive index of the samples increases rapidly when the molar fraction of titanium dioxide varies from 45% to 53%.

The  $v_d$  (Abbe number) of the glasses can be calculated according to the following formula:  $v_d = (n_d - 1) / (n_F - n_C)$ , where  $n_d$ ,  $n_F$ , and  $n_C$  are the refractive indices at 587.6, 486.1, and 656.3 nm, respectively. The value of  $v_d$  initially increases and reaches a maximum value of 22.56 for GLT-4 glass. For the GLT-(1-5) glasses,  $v_d$  shows a downward trend. With an increase in the refractive index, the Abbe number shows an opposite trend.

## 2.4 Glass density, molar volume, and oxygen ion polarizability

Density, an important physical property of glasses, is closely related to the structure and composition. It reflects parameters such as the molecular weight, coordination number of atoms, and packing density of the glasses. The density is measured using the gas expansion replacement method. The volume of the glass samples is measured. The volume is obtained after 15 times of test. The samples' density  $\rho$  can be obtained after weighing the mass of the samples.

According to Fig. 6, the density of GLT glasses decreases gradually with the increase in TiO<sub>2</sub> content. The density decreases from 5.06 to 5.00 g/cm<sup>3</sup>. The content of TiO<sub>2</sub> is increased by 6% (in mol), while the density is decreased by 0.06 g/cm<sup>3</sup>, indicating a significant effect on the density. The effect of composition on the density can be explained in three aspects.

Firstly, the molecular weight of GeO<sub>2</sub> is 104.64. As TiO<sub>2</sub> shows a comparatively small molecular weight of only 79.87, the density decreases after TiO<sub>2</sub> replaces GeO<sub>2</sub>. Secondly, from the view of atomic stacking, a different oxygen content can result in a different molecular

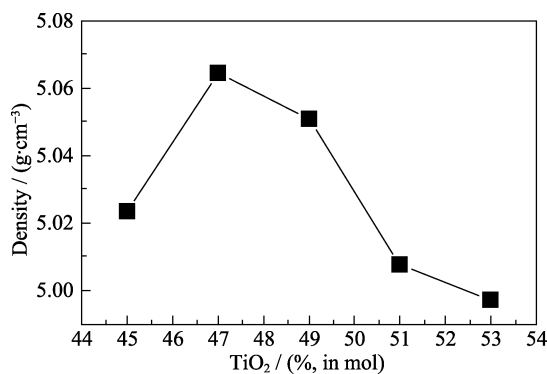


Fig. 6 Dependence of density of GLT-(1-5) glasses on glass compositions

structure. The tighter network structure can cause a higher atomic packing density, showing a higher density. The last aspect is the coordination number of metal ions, which is an important structural feature of glasses. The coordination number of La<sup>3+</sup> is 9<sup>[29]</sup>, which is higher than that of general Ge<sup>4+</sup> (4 or 6)<sup>[30]</sup>. A denser glass network structure can be obtained by a higher coordination number so that the density increases with an increase in La<sup>3+</sup> and decrease in Ge<sup>2+</sup>. Generally, Ti<sup>4+</sup> ions have 4, 6 coordination number, which is similar to germanium. The contribution to the density of the network structure is roughly the same. However, its relative molecular weight is small. Therefore, the density of the GLT-(1-5) glasses decreases with an increase in the TiO<sub>2</sub> content.

The variation law of the refractive index is discussed in relation with the content of metal ions, according to Lorentz-Lorenz formula<sup>[31]</sup>:

$$\frac{n^2 - 1}{n^2 + 2} \frac{M}{\rho} = \frac{n^2 - 1}{n^2 + 2} V_m = R_m = \frac{4\pi}{3} \sum_i N_i \alpha_i \quad (1)$$

$$V_m = M / \rho \quad (2)$$

where  $M$  is the relative molecular weight of the oxide component and  $\rho$  is the density of the glass sample.  $n$  represents the refractive index of the material,  $N_i$  represents the number of  $i$  atoms, and  $\alpha_i$  represents the electron polarizability of  $i$  atoms. And  $V_m$  and  $R_m$  represent the molar volume of the material and the molecular refractive index of the material, respectively. The formula shows that the molar volume  $V_m$  and electronic polarizability  $\alpha_i$  are two important factors affecting the refractive index<sup>[32]</sup>. In the oxide system, the polarizability of the metal ions is very weak compared to that of oxygen ions. The effect on the refractive index is negligible. Therefore, we only discuss the electronic polarizability of oxygen ions. When the TiO<sub>2</sub> content is more than 49% (in mol), the calculated molar volume of the GLT glasses, listed in Table 1, is increased with the increase of TiO<sub>2</sub> content. Then, the electron polarization rate of oxygen,  $\alpha_o$ , is obtained by the deformed derivation of the Lorentz-Lorenz formula<sup>[33-34]</sup>. The calculation formula of  $\alpha_o$  is as follows:

$$\alpha_o = [(V_m / 2.52)(n^2 - 1) / (n^2 + 2) - \sum a_i] (N_o)^{-1} \quad (3)$$

In GLT glasses, the polarizabilities of metal cationic La<sup>3+</sup>, Ge<sup>4+</sup>, and Ti<sup>4+</sup> are 1.04, 0.143, and 0.185<sup>[2]</sup>, respectively. The uncertainty of molar volume  $V_m$  and electronic polarizability  $\alpha_i$  is affected by refractive index and density. The uncertainty is  $\pm 0.015$ .

Clearly, the molar volume  $V_m$  and oxygen electron polarizability  $\alpha_i$  gradually increase with an increase in TiO<sub>2</sub>, similarly to the refractive index of the glass samples.

**Table 1** Density, molar volume and oxygen ions polarizability of GLT-(1–5) glasses

Sample	TiO <sub>2</sub> content/ % (in mol)	Weight, m/g	True density, $\rho/(\text{g}\cdot\text{cm}^{-3})$	Molar volume, $V_m/(\text{cm}^3\cdot\text{mol}^{-1})$	Electron polarizability of oxygen, $\alpha_O/(\times 10^{-3}, \text{nm}^3)$
GLT-1	45	4.8063	5.02	30.06	2.388
GLT-2	47	4.4328	5.06	29.72	2.389
GLT-3	49	4.5602	5.05	29.67	2.406
GLT-4	51	4.2007	5.01	29.86	2.406
GLT-5	53	4.7872	5.00	29.82	2.420

### 3 Conclusions

GeO<sub>2</sub>-La<sub>2</sub>O<sub>3</sub>-TiO<sub>2</sub> glasses with large size and high refractive index were successfully prepared by high-temperature melting-quenching method. Thermal and optical property of the glasses were researched. The maximum  $\Delta T$  can reach 236 °C, indicating high glass forming ability and strong resistance to crystallization. The maximum refractive index  $n_d$  and Abbe number reach 2.06 and 23, respectively. 49% (in mol) is the optimal TiO<sub>2</sub> concentration for the glass stability. The glass forming ability and thermal stability can be weakened by increasing the content of TiO<sub>2</sub> in GLT-(1–5). In contrast, the refractive index has been significantly improved. The refractive index is affected by glass compositions, coordination number of metal ions, polarizability of oxygen ions, and structure of the glass network. The molar volume  $V_m$  and oxygen electron polarizability  $\alpha_i$  have the same variation trend as the refractive index of the glass samples. For lanthanum titanium glass prepared by high-temperature melting method, the increase of titanium content can effectively increase the refractive index of the glass, and still maintain a high transmittance in the visible light band. As a result of the good thermal and optical property, the GLT glasses can be used in optical windows and lenses under high temperature conditions.

### References:

- [1] XIE J, ZHANG M, GUO R, *et al.* Investigation of optical and thermal properties in Er<sup>3+</sup>-doped Ga<sub>2</sub>O<sub>3</sub>-La<sub>2</sub>O<sub>3</sub>-Ta<sub>2</sub>O<sub>5</sub> glasses fabricated by containerless solidification. *Journal of Alloys and Compounds*, 2021, **872**: 159651.
- [2] CAURANT D, GOURIER D, PRASSAS M. Electron-paramagnetic-resonance study of silver halide photochromic glasses: darkening mechanism. *Journal of Applied Physics*, 1992, **71(3)**: 1081.
- [3] KANEKO M, YU J, MASUNO A, *et al.* Glass formation in LaO<sub>3/2</sub>-TiO<sub>2</sub> binary system by containerless processing. *Journal of the American Ceramic Society*, 2012, **95(1)**: 79.
- [4] MASUNO A, WATANABE Y, INOUE H, *et al.* Glass-forming region and high refractive index of TiO<sub>2</sub>-based glasses prepared by containerless processing. *Physica Status Solidi (c)*, 2012, **9(12)**: 2424.
- [5] ZHANG J, ZHANG X, LI Y, *et al.* High-entropy oxides 10La<sub>2</sub>O<sub>3</sub>-20TiO<sub>2</sub>-10Nb<sub>2</sub>O<sub>5</sub>-20WO<sub>3</sub>-20ZrO<sub>2</sub> amorphous spheres prepared by containerless solidification. *Materials Letters*, 2019, **24**: 167.
- [6] ARAI Y, ITOH K, KOHARA S, *et al.* Refractive index calculation using the structural properties of La<sub>4</sub>Ti<sub>9</sub>O<sub>24</sub> glass. *Journal of Applied Physics*, 2008, **103(9)**: 094905.
- [7] GREGOR R B, LYTLE F W, SANDSTROM, *et al.* Investigation of TiO<sub>2</sub>-SiO<sub>2</sub> glasses by X-ray absorption spectroscopy. *Journal of Non-Crystalline Solids*, 1983, **55(1)**: 27.
- [8] CORMIER L, GASKELL P H, CALAS G, *et al.* Medium-range order around titanium in a silicate glass studied by neutron diffraction with isotopic substitution. *Physical Review B*, 1998, **58(17)**: 11322.
- [9] FARGES F, BROWN G E, NAVROTSKY A, *et al.* Coordination chemistry of Ti(IV) in silicate glasses and melts: II. Glasses at ambient temperature and pressure. *Geochimica et Cosmochimica Acta*, 1996, **60(16)**: 3039.
- [10] DUOERKUN G, ZHANG Y, SHI Z, *et al.* Construction of n-TiO<sub>2</sub>/p-Ag<sub>2</sub>O junction on carbon fiber cloth with VIS-NIR photore-sponse as a filter-membrane-shaped photocatalyst. *Advanced Fiber Materials*, 2020, **2(1)**: 13.
- [11] SUN Y, MWANDEJE J B, WANGATIA L M, *et al.* Enhanced photocatalytic performance of surface-modified TiO<sub>2</sub> nanofibers with rhodizonic acid. *Advanced Fiber Materials*, 2020, **2(5)**: 118.
- [12] MAO Z Z, DUAN J, ZHENG X J, *et al.* Study on optical properties of La<sub>2</sub>O<sub>3</sub>-TiO<sub>2</sub>-Nb<sub>2</sub>O<sub>5</sub> glasses prepared by containerless processing. *Ceramics International*, 2015, **41(S1)**: S51.
- [13] LI Y, ZHANG X, QI X, *et al.* High refractive index LaGaO<sub>3</sub>-TiO<sub>2</sub> amorphous spheres prepared by containerless solidification. *Materials Letters*, 2018, **215**: 148.
- [14] HAN J, WANG Z, LI J, *et al.* Large-sized La<sub>2</sub>O<sub>3</sub>-TiO<sub>2</sub> high refractive glasses with low SiO<sub>2</sub> fraction by hot-press sintering. *International Journal of Applied Glass Science*, 2019, **10(3)**: 371.
- [15] HUANG S J, XIAO Y B, LIU J L, *et al.* Nd<sup>3+</sup>-doped antimony germanate glass for 1.06 μm fiber lasers. *Journal of Non-Crystalline Solids*, 2019, **518**: 10.
- [16] KAMITSOS E I, YIANNPOULOS Y, KARAKASSIDES N M A, *et al.* Raman and infrared structural investigation of xRb<sub>2</sub>O-(1-x)GeO<sub>2</sub> glasses. *The Journal of Physical Chemistry*, 1996, **100(28)**: 11755.
- [17] WANG L L, GUO Y Y, GAO C M, *et al.* Preparation and spectral properties of Ho<sup>3+</sup>/Tm<sup>3+</sup> co-doped germanium glass active optical fiber material. *Proceedings of SPIE--The International Society For Optical Engineering*, 2014(**9295**): 92950F.
- [18] LIU H, GE X, HU Q, *et al.* A new sight into the glass forming ability caused by doping on Ba-and Ti-site in BaTi<sub>2</sub>O<sub>5</sub> glass. *Journal of Materials Science & Technology*, 2020, **54(19)**: 112.
- [19] RAJINDER K, ATUL K, MARINA G B, *et al.* Structural, thermal and optical characterization of co-existing glass and anti-glass phases of xLa<sub>2</sub>O<sub>3</sub>-(100-x)TeO<sub>2</sub> and 2TiO<sub>2</sub>-xLa<sub>2</sub>O<sub>3</sub>-(98-x)TeO<sub>2</sub> systems. *Journal of Non-Crystalline Solids*, 2020, **540(C)**: 120117.
- [20] CHEN D D, LIU Y H, ZHANG Q Y, *et al.* Thermal stability and spectroscopic properties of Er<sup>3+</sup>-doped niobium tellurite glasses for broadband amplifiers. *Materials Chemistry and Physics of Applied Physics*, 2005, **90(1)**: 78.

- [21] CHUMAKOV A I, MONACO G, FONTANA A, *et al.* Role of disorder in the thermodynamics and atomic dynamics of glasses. *Physical Review B: Condensed Matter & Materials Physics*, 2014, **112(2)**: 025502.
- [22] WANG W H. Dynamic relaxations and relaxation-property relationships in metallic glasses. *Progress in Materials Science*, 2019, **106(C)**: 100561.
- [23] ZHANG L Y, LI H, HU L L. Statistical structure analysis of GeO<sub>2</sub> modified Yb<sup>3+</sup>-phosphate glasses based on Raman and FTIR study. *Journal of Alloys and Compounds*, 2017, **698**: 103.
- [24] CAO W, HUANG F, YE R, *et al.* Structural and fluorescence properties of Ho<sup>3+</sup>/Yb<sup>3+</sup> doped germanosilicate glasses tailored by Lu<sub>2</sub>O<sub>3</sub>. *Journal of Alloys and Compounds*, 2018, **746**: 540.
- [25] FAN X, LI K, LI X, *et al.* Spectroscopic properties of 2.7 μm emission in Er<sup>3+</sup> doped telluride glasses and fibers. *Journal of Alloys and Compounds*, 2014, **615**: 475.
- [26] YOSHIHIRO A, DAVIDE C. Determination of combined water in glasses by infrared spectroscopy. *Journal of Materials Science Letters*, 2004, **9(2)**: 244.
- [27] HARRISON A J. Water content and infrared transmission of simple glasses. *Journal of the American Ceramic Society*, 1947, **30(12)**: 362.
- [28] HIROTA S, IZUMITANI T. Effect of cations on the inherent absorption wavelength and the oscillator strength of ultraviolet absorptions in borate glasses. *Journal of Non-Crystalline Solids*, 1978, **29(1)**: 109.
- [29] REN G, CAO W, LEI R, *et al.* Observation of efficient Er<sup>3+</sup>: <sup>4</sup>I<sub>11/2</sub> → <sup>4</sup>I<sub>13/2</sub> transition in highly Er<sup>3+</sup> doped germanosilicate glass. *Ceramics International*, 2018, **44(14)**: 16868.
- [30] INOUE H, WATANABE Y, MASUNO A, *et al.* Effect of substituting Al<sub>2</sub>O<sub>3</sub> and ZrO<sub>2</sub> on thermal and optical properties of high refractive index La<sub>2</sub>O<sub>3</sub>-TiO<sub>2</sub> glass system prepared by containerless processing. *Optical Materials*, 2011, **33(12)**: 1853.
- [31] ERSUNDU A E, ÇELIKBILEK M, BAAZOUZI M, *et al.* Characterization of new Sb<sub>2</sub>O<sub>3</sub>-based multicomponent heavy metal oxide glasses. *Journal of Alloys and Compounds*, 2014, **615(C)**: 712.
- [32] DIMITROV V, KOMATSU T. Electronic polarizability, optical basicity and non-linear optical properties of oxide glasses. *Journal of Non-Crystalline Solids*, 1999, **249(2)**: 160.
- [33] YOSHIMOTO K, MASUNO A, INOUE H, *et al.* Transparent and high refractive index La<sub>2</sub>O<sub>3</sub>-WO<sub>3</sub> glass prepared using containerless processing. *Journal of the American Ceramic Society*, 2012, **95(11)**: 063520.
- [34] MASUNO A, INOUE H, YU J, *et al.* Refractive index dispersion, optical transmittance, and Raman scattering of BaTi<sub>2</sub>O<sub>5</sub> glass. *Journal of Applied Physics*, 2010, **108(6)**: 1081.

## GeO<sub>2</sub>-La<sub>2</sub>O<sub>3</sub>-TiO<sub>2</sub> 玻璃的结构、热学和光学性质

万家宝<sup>1</sup>, 张明辉<sup>2</sup>, 苏怀宇<sup>2</sup>, 曹枝军<sup>2</sup>, 刘学超<sup>2</sup>,  
谢坚生<sup>2</sup>, 王祥远<sup>2</sup>, 时英辉<sup>2</sup>, 王亮<sup>2</sup>, 雷水金<sup>1</sup>

(1. 南昌大学 物理与材料学院, 南昌 330031; 2. 中国科学院 上海硅酸盐研究所, 上海 200050)

**摘要:** La<sub>2</sub>O<sub>3</sub>-TiO<sub>2</sub> 玻璃以其折射率高、光学性能优异, 在透镜、光学窗口、光通信等领域具有广阔的应用前景。受限于玻璃形成能力, 人们难以制备出大尺寸 La<sub>2</sub>O<sub>3</sub>-TiO<sub>2</sub> 玻璃, 这严重限制其应用。本研究通过引入网络形成体 GeO<sub>2</sub>, 有效提高了玻璃形成能力, 从而可用常规方法制备大尺寸的 GeO<sub>2</sub>-La<sub>2</sub>O<sub>3</sub>-TiO<sub>2</sub>(GLT)玻璃。差热分析表明, GLT 玻璃具有较高的玻璃转变温度和抗析晶性能, 玻璃转变温度  $T_g$  和  $\Delta T$  ( $\Delta T = T_{c-onset} - T_g$ ) 分别大于 833 和 209 °C。最大折射率为 2.06, 在可见光和近红外波段的透过率可达 78%。实验还研究了 Ti 含量对 GLT 玻璃结构、热学和光学性能的影响。结果表明, 随着钛含量增加, 玻璃的形成能力和热稳定性均减弱。摩尔体积  $V_m$  和氧离子极化率  $\alpha_i$  的变化趋势与折射率一致。GLT 玻璃对开发高性能、轻量化、小尺寸的新型器件具有重要意义。

**关键词:** 高折射率; 热稳定性; 大尺寸玻璃; 高透过率

**中图分类号:** TQ171 **文献标志码:** A